Consensus Strategy for State-Aware Coordination of Renewable Energy Sources and Battery Storage Systems in Islanded DC Microgrids

Mohammad Amin Rezaei[1], Mohammad Rajabi Nasab[1], Luca De Cicco[1], Silviu-Iulian Niculescu[2], Arben Cela[3], Saverio Mascolo[1], Marco Liserre[4]

***Abstract*—Islanded DC microgrids relying on Renewable Energy Sources (RESs), such as photovoltaic and wind systems, face significant challenges in maintaining stable operation due to the intermittent nature of renewable generation and the uncertainty of demand. To address this issue, energy storage systems (battery stacks) are typically integrated to balance supply and demand over different time scales. Effective coordination of these components is therefore essential for reliable long-term operation. This paper proposes a consensus-based control approach that coordinates in-service batteries to share power imbalances when RES generation, operating with the Maximum Power Point Tracking (MPPT) algorithm, does not match the load demand. By driving the batteries' State of Charge (SoC) to consensus, the proposed method improves their performance and lifespan, while ensuring that the load demand is satisfied. In scenarios where all the batteries are fully charged, Cpower redistribution among RES units is employed to preserve the supply–demand balance. Simulation results confirm the effectiveness of the presented method in achieving SoCs consensus under different operating conditions. In addition, a realistic converter transfer function model is incorporated to validate the proposed control strategy.**

Index terms: *Consensus, multi-agent systems, microgrid, SoC balancing, energy management.*

I. Introduction

The increasing penetration of Renewable Energy Sources (RESs), particularly solar and wind, is transforming modern power systems from centralized generation toward decentralized architectures. In this context, DC Microgrids (DC-MGs) allow efficient integration of components with inherently DC characteristics, such as most RESs and domestic loads, as well as Energy Storage Systems (ESSs) [1]. Fig. 1 shows a generic structure of an isolated DC-MG. Isolated DC microgrids can be found in applications such as remote telecom sites, data centers, off-grid residential or industrial areas [2]. This paradigm reduces energy losses by eliminating multiple conversion stages. Moreover, the absence of frequency, reactive power, and grid synchronization requirements simplifies DC-MG control [3].

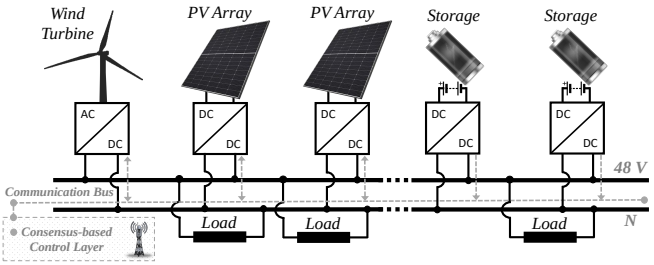

Fig. 1: A typical islanded DC-MG.

In modern stand-alone DC-MGs that rely on intermittent RESs, maintaining reliable operation remains a primary challenge. The inherent variability of these sources can exacerbate the mismatch between supply and demand [2]. Since the system's power balance primarily affects the common bus voltage, this equilibrium must be maintained in real time to keep the bus voltage close to its nominal value [4]. To address this issue, Battery Energy Storage Systems (BESSs) can be employed, due to their capability to support bidirectional energy flow.

However, when multiple BESSs are connected in parallel, it is desirable for batteries with different capacities and initial SoC levels to contribute to power compensation according to their unit-specific characteristics so that their SoC differences can be gradually equalized over time. Achieving such SoC balancing is important to minimize the depth of discharge of individual batteries and to prevent overcharging or deep discharging leading to a longer service life [5].

When multiple generation units operate within the DC-MG, it is generally desirable to work in MPPT mode to harvest all available power. However, it is not always applicable in isolated entities, as it may lead to an unmanageable excess of energy [6]. Therefore, in cases of excessive generation with fully charged batteries, there should be an option to curtail the power and manage the supply to match demand. To this end, different ratings of RESs should also be taken

[1]Department of Electrical and Information Engineering, Politecnico di Bari, Italy. m.rezaeinaghadehi@phd.poliba.it, m.rajabinasab@phd.poliba.it, {luca.decicco, saverio.mascolo}@poliba.it

[2]University Paris-Saclay, CNRS, CentraleSupélec, Inria, Laboratory of Signals and Systems (L2S), Gif-sur-Yvette, France. silviu.niculescu@centralesupelec.fr

[3]Universite Gustave Eiffel, Department of Computer Science and Telecommunications, Laboratory of Images, Signals and Intelligent Systems (LISSI), France. arben.cela@esiee.fr

[4]Chair of Power Electronics, Department of Electrical and Information Engineering, University of Kiel, Germany. ml@tf.uni-kiel.de

into account in determining their participation in power provision [5]. This consideration is essential to extend the lifetime of each unit by avoiding overgeneration and preventing thermal stress on the converters of smaller units [7]. Thus, besides voltage regulation, SoC management of batteries, and current sharing among in-service units are crucial for safe and reliable operation of the microgrid [8]. For this purpose, coordinated operation of the units is required.

Consensus-based control is the natural control tool to design cooperative energy management in islanded microgrids [9]. Consensus algorithms can coordinate energy sources through local communication to achieve objectives such as voltage regulation, efficient battery operation, power sharing, and minimized energy cost without relying on intensive commputation units [10]. Consensus-based control offers faster computations compared to optimization-based controllers, and improved situational awareness compared to conventional controllers, by taking advantage of communication among agents.

Consensus-tracking methods have been applied to coordinate the SoC of heterogeneous storage units while simultaneously maintaining voltage and frequency stability [11]. However, most existing studies assume that PV units operate in a fixed mode, typically under MPPT. In this work, a more realistic control strategy is proposed, considering all possible operating modes of the DC-MG while accounting for the unit-specific characteristics of the batteries and RESs to achieve an accurate power distribution among the units.

However, employing a standard consensus protocol to coordinate the batteries is not suitable since, once batteries are active, it causes circular currents among the batteries and wastes energy [12]. To solve this issue, a modified consensus algorithm is proposed that avoids such energy flows among BESSs during replenishment. Hence, the demanded load will be energized by the RES units and supported by batteries, and the batteries with low SoC will only be charged by the RES units once the RESs' MPPT-based generation exceeds the demand.

Based on the above discussion, this paper proposes a modified consensus-based control strategy for SoC coordination of heterogeneous batteries in islanded DC-MGs with RES units. By including unit-specific data of the batteries and RESs, the proposed approach aims to propose an energy management approach that provides proper flexibility while covering all possible operating modes of the DC-MG. Here, RESs operate in the MPPT phase as the primary controllers of the system, while the batteries are activated in charging/discharging mode depending on the supply–demand conditions. In the case of surplus generation of MPPT-based RESs and fully charged batteries, the RES units will be switched from MPPT to load-sharing mode in order to preserve the supply–demand balance. To the best of the authors' knowledge, the proposed approach introduces a new strategy for state-aware coordination of battery storage and RESs in islanded DC-MGs. Moreover, the provided method has been validated with a real converter.

The remainder of the paper is organized as follows: Section II provides some preliminaries, Section III presents the problem formulation for the proposed consensus algorithm, dynamics and operational modes, and the DC-bus signaling approach used to derive the deficit/surplus current for battery coordination. Simulations are presented in Section IV and Section V concludes the paper.

II. Preliminaries

This section provides the necessary notation employed in the problem formulation. An undirected graph $G(\mathcal{V}, \mathcal{E})$, where $\mathcal{V} = \{v_1, \ldots, v_N\}$ is the set of nodes, and $\mathcal{E} \subseteq \mathcal{V} \times \mathcal{V}$ is the set of edges. An edge (v_i, v_j) denotes the information flow from node i to node j. The set of neighbours of node v_i is defined as $\mathcal{N}_i = \{v_j \in \mathcal{V} : (v_j, v_i) \in \mathcal{E}\}$. The adjacency matrix A, associated with a graph, represents the connections of the nodes. In other words, $A = (a_{ij})$ is such that $a_{ij} = 1$ if $(i, j) \in \mathcal{E}$ and $a_{ij} = 0$ otherwise. Let $D(G) = (d_{ij})$ be the degree matrix with $d_{ij} = \deg(v_i)$ if $i = j$ and $d_{ij} = 0$ otherwise, where $\deg(v_i)$ is the number of edges connected to node v_i. The Laplacian matrix is defined as $L = D - A$. A graph is connected if a path exists from each node to every other node, and a graph is fully connected if there is a direct path between every pair of nodes.

III. Problem definition

This section introduces the consensus algorithm proposed in this work, the microgrid's possible operating modes, and some useful remarks highlighting related key aspects.

A. Consensus Algorithm

Consensus is a widely used method for MAS in which the states/outputs of the agents reach the same value [13]. This state can represent a variety of concepts, including currents and voltages [14], the position of drones [15], etc. For a continuous-time system, the consensus algorithm is defined as follows.

Definition 1. *A set of agents of a multi-agent system reaches consensus in their states if and only if:*

$$\lim_{t \to \infty} (x_i(t) - x_j(t)) = 0. \tag{1}$$

The necessary and sufficient condition for reaching consensus is to have a connected underlying communication graph. However, we assume to have a fully connected communication network among the in-service units. To model the dynamics of each of the batteries, a single integrator in discrete-time domain is used in (2):

$$x_i(k+1) = x_i(k) + T_s u_i(k) \tag{2}$$

Here, x_i, T_s, u_i are the sate, sampling time, and control input, respectively. To achieve consensus among the agents, the control input is as follows:

$$u_i(k) = g \sum_{j \in \mathcal{N}_i} a_{ij}(x_j(k) - x_i(k)) \tag{3}$$

where a_{ij} are the elements of the adjacency matrix A, and $g \in \mathbb{R}$ is a positive control gain that must satisfy $0 < g \leq \frac{1}{D_{\max}}$ to lead to consensus [9]. The quantity $D_{\max} > 0$ denotes the maximum degree of a node in the degree graph.

B. Dynamics and Operating Modes

The SoC of a battery in an islanded grid is defined based on the current that charges/discharges it, the sampling time, the capacity of the battery, and the initial SoC, which is known as the Coulomb Counting Method [16]. For a discrete-time dynamical model, the dynamics of the SoC is given by:

$$SoC_i(k+1) = SoC_i(k) - \frac{\Delta T \cdot I_i(k)}{3600 \cdot C_i}, \qquad i = 1, \ldots, N, \tag{4}$$

where N is the number of batteries, ΔT is the sampling time, and SoC_i, C_i, and I_i are the state of charge, capacity (Ampere-hours, Ah), and reference current of battery i, respectively. Based on this formulation, if I_i is positive (negative), the battery discharges (charges), meaning that the SoC decreases (increases). Four different operating modes are possible based on the amount of generated energy and consumption.

Mode 1: When the demanded power is equal to the power generated by the RES units; therefore, the BESSs remain out of service in this operating condition.

Mode 2: When the demanded power exceeds the total power generated by the MPPT-based RES units, the batteries must compensate for the deficit to meet the demanded load.

Mode 3: When the demanded power is lower than the power generated by the MPPT-based RES units the batteries are activated to act as additional loads and absorb the surplus energy.

Mode 4: Once the BESSs are fully charged, they can no longer operate as additional loads. If generation still exceeds the demand, the voltage of the common bus begins to rise. To prevent it, the RESs exit the MPPT mode and switch to load-sharing control, thereby reducing their power generation and regulating the common bus voltage.

Note that in Mode 4, the currents of the RES units will be decreased to meet the demanded energy; therefore, they are no longer in MPPT mode. The division of the currents is based on the maximum currents that each of the RES units can supply. Aside from Mode 1, which is the ideal mode, the remaining working modes can happen in two different cases, as follows.

Case 1. *The SoCs are the same for the batteries.*

For this case, there is no need to run a consensus algorithm for the batteries, and the charging/discharging will be based on their capacities. Of course, this process should be carried out to keep the SoCs the same over the operation time. Based on (4), we have:

$$Soc_i(k) - \frac{\Delta T I_i(k)}{3600 \cdot C_i} = Soc_j(k) - \frac{\Delta T I_j(k)}{3600 \cdot C_j} \tag{5}$$

Since SoCs are equal, one can write equation (5) as follows:

$$\frac{I_i(k)}{C_i} = \frac{I_j(k)}{C_j} \tag{6}$$

Considering and extending (6), the reference current when the SoCs are the same is as follows:

$$I_i(k) = \frac{I_{\text{error}}(k) C_i}{\sum_{j=1}^{N} C_j}, \tag{7}$$

where $I_{\text{error}} = I_{\text{demand}} - \sum_{i=1}^{M} I_{\text{RES}_i}$ (M is the number of RES units). Using this simple formula for the currents of the batteries, the SoCs will remain the same for all the batteries. Note that I_{error} can be negative/positive, which causes the batteries to charge/discharge, respectively. I_{demand} is the required current that must be provided by the sources to preserve the common bus voltage at its nominal value. This value can be determined using the DC bus signaling technique [4], which is described in the following subsection.

Case 2. *The SoCs are not the same for the batteries.*

In this case, the consensus algorithm must be run for the batteries to reach the same values of SoC, as well as to discharge/charge the batteries with a suitable proportion of the currents to respect the capacities of the batteries. Consider the consensus formula for the case of SoCs (8):

$$Soc_i(k+1) = Soc_i(k) + g \sum_{j \in N_i} a_{ij} (Soc_j(k) - Soc_i(k)) \tag{8}$$

Based on (4) and (8), one can compute the values of the currents that discharge/charge the batteries to reach consensus on the SoCs. In (8), the control input is the difference between SoCs, which needs to be translated into the required current from the battery. This can be done using (4) and (8) as follows.

$$g \sum_{j \in N_i} a_{ij} \big(Soc_j(k) - Soc_i(k)\big) = -\frac{\Delta T \cdot I_{Soc_i}(k)}{3600 \cdot C_i}$$

$$I_{Soc_i}(k) = (-\frac{3600 \cdot C_i}{\Delta T})(g \cdot \sum_{j \in N_i} a_{ij} \big(Soc_j(k) - Soc_i(k)\big)) \tag{9}$$

where I_{SoC_i} is the current needed to compensate for the difference in the SoC. I_{SoC_i} and I_{error} will be used to compute the reference current of each battery, I_i. Note that I_{SoC_i} can be a large current because of the nature of the relationship between the current and the SoC of a battery. Let us define $\Delta_i = g \sum_{j \in \mathcal{N}_i} a_{ij} \big(SoC_j(k) - SoC_i(k)\big)$. From (9), one can notice the large value of $3600 \cdot C_i$, which is natural since the SoC of a battery changes slowly while charging/discharging. Therefore, this paper suggests to compute the reference current for each battery as in (10).

TABLE I: Characteristics of the tested DC-MGs.

Parameters	Symbol	Value
Nominal Voltage	V_{nom}	48 V
Max. Current (PV_1 & PV_2)	I_{max}	10 A
Max. Current ($Wind\ Turbine$)	I_{max}	5 A
Common Bus Capacitance	C_{bus}	20 mF

$$I_i(k) = \begin{cases} \dfrac{I_{Soc_i}(k)}{\sum_{j=1}^{N} I_{Soc_j}(k)} I_{\text{error}} & I_{\text{error}}\Delta_i < 0, \\ 0 & else. \end{cases} \tag{10}$$

The first condition refers to the fact that the signs of I_{error} and Δ_i must be different. For instance, when I_{error} is positive (negative), it means that the batteries should deliver (absorb) current; however, only those batteries should participate that have a negative (positive) Δ_i, which means that they have a greater (smaller) SoC with respect to the others.

C. DC Bus signaling

As stated in Section I, the DC common-bus voltage (i.e., V_{bus}) reflects the power balance condition of the microgrid. This is because a generation deficit discharges the equivalent DC-bus capacitor, causing a voltage drop, whereas surplus generation charges it, resulting in a voltage rise. This correlation between the common-bus equivalent capacitance and the voltage deviation determines the proper value of I_{error}, the parameter that specifies the surplus or deficit current to be compensated by the batteries. Irrespective of the operating mode of the microgrid, the common-bus voltage is modeled as:

$$V_{bus} = \frac{1}{C_{bus}} \int_{t_0}^{t} \left(I_{\text{demand}} - \sum_{i=1}^{M} I_{RES_i} \right) dt \tag{11}$$

where C_{bus} is the common bus capacitance. Assuming an ideal controller, an ideal battery (with negligible terminal-voltage variation across different SoC levels), and considering the demonstration in [17] that line resistances can be designed to ensure negligible voltage drops, the dynamic behavior of V_{bus} can be obtained by solving the previous differential equation, given by:

$$V_{\text{bus}}(t) = V_{\text{bus}}(t_0) + \frac{I_{\text{demand}} - \Sigma_{i=1}^{M} I_{RES_i}}{C_{\text{bus}}} (t - t_0), \tag{12}$$

Thus, V_{bus} changes linearly with time, with the slope of $(I_{\text{demand}} - \Sigma_{i=1}^{M} I_{RES_i})/C_{\text{bus}}$. Under normal conditions, $V_{\text{bus}}(t_0) = V_{nom}$. In steady-states, the voltage deviation from its nominal value (i.e., $\Delta V = \lim_{t\to\infty} V_{bus}(t) - V_{nom}$) is zero provided that the supply satisfies the demand, denoted as $I_{\text{error}} = 0$. Otherwise, I_{error} can be computed from the resulting voltage deviation at the common bus as well as the sum of measured terminal currents of i-th RES, as shown in (12).

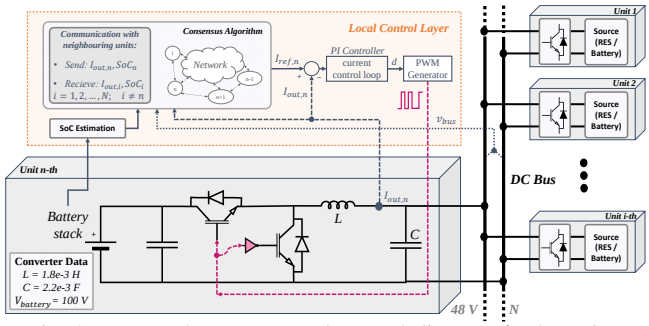

Fig. 2: Proposed converter and control diagram for batteries.

D. Converter and Controller Diagram

As shown in Fig. 2, the local controller layer receives the information regarding SoCs, currents, and bus voltage to compute the reference current for the SoC consensus among the storage units. Using a PI controller, the error between the battery and reference current is used to provide the needed duty cycle. This duty cycle will then be applied to a Pulse Width Modulation (PWM) generator to control the battery current by manipulating the corresponding converter, and eventually, leading to voltage regulation and SoC consensus among the batteries. The converter transfer function based on this elaboration can be determined as follows:

$$G_{Converter} = \frac{I_{Battery}}{DutyCycle} \frac{1 + r_C C s}{LCs^2 + (\frac{L}{R} + (r_L + r_C)C)s + (1 + \frac{r_L}{R})} \tag{13}$$

where C and L represent the capacitance and inductance of the converter output filter, respectively, and R is the total load connected to the bus. The parameters r_C and r_L stand for the Equivalent Series Resistances (ESRs) of the filter capacitor and the inductor, respectively which are included to model the converter more realistically [18].

IV. Simulation Results

In this section, the simulation results for the consensus among the SoCs, and charge/discharge currents of the batteries have been illustrated. Three different examples have been covered to show different operation modes of the islanded grid.

1) Example 1: In this example, modes 1,2, and 3 has been simulated. For the initial parameters, we considered $N = 5$ batteries with initial SoCs of $SoC = [0.9, 0.5, 0.7, 0.8, 0.6]$, zero initial currents from the batteries, capacities as $Cap = [50, 100, 150, 200, 250]Ah$, $g = 0.2$, and $\Delta T = 1s$. The simulation runtime is 86400 seconds (a full day). The demanded energy from the grid, and the produced energy from RESs are time-varying. Due to changes in sunlight and wind, neither RESs produce constant energy, nor do consumers use constant energy during the day. Fig. 3 shows I_{demand}, I_{RES}, and I_{error} representing a logical operating mode for a full day.

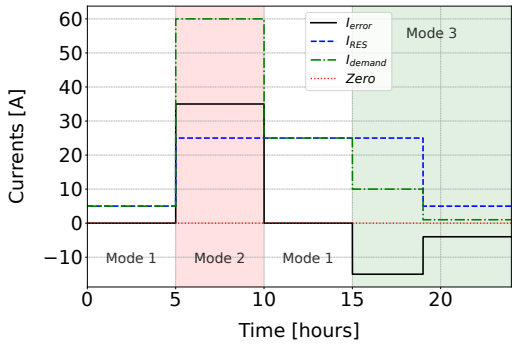

Fig. 3: Demanded and produced currents in a day.

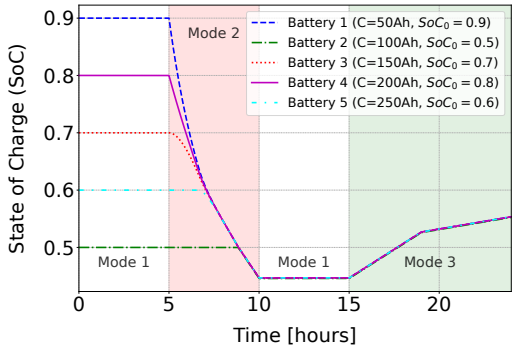

Fig. 4: Consensus of the SoCs for $N = 5$ batteries

Fig. 4 shows the consensus of the SoCs for the batteries. Starting from the initial SoCs, they reach consensus and then continue to discharge/charge based on the demanded and produced energy. Obviously, battery 2 does not participate in the consensus until 8 hours due to the positive I_{error} and its negative Δ_i as in (10).

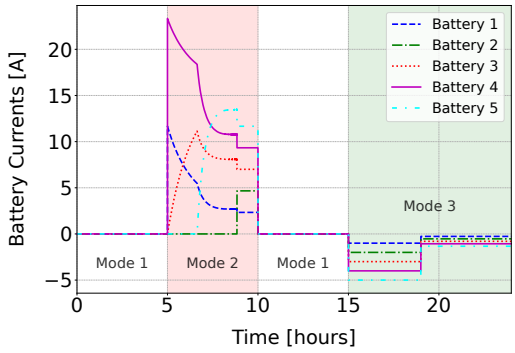

Fig. 5: Battery currents for $N = 5$ batteries

Fig. 5 shows the coordinated charge/discharge currents for the $N = 5$ batteries based on the demanded and produced energy.

2) Example 2: Consider that the amount of produced energy is more than the demanded one; so, the batteries are full and they cannot absorb the exceeded energy. As mentioned in Mode 4, the RES units reduce their production in order to meet the demanded energy. Initial conditions are the same except for $Cap = [50, 100, 150, 200, 250]Ah$. Fig. 6 shows the SoCs of the batteries in which all of them have reached 1 while they are in Mode 3.

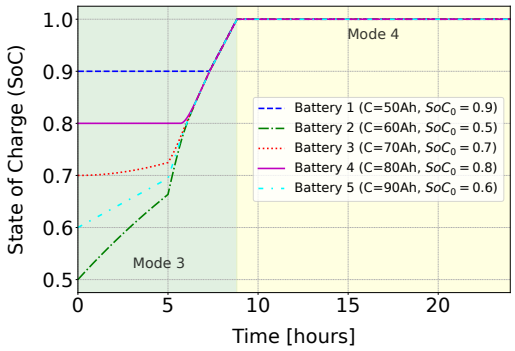

Fig. 6: SoC consensus in Mode 4 for $N = 5$ batteries

Fig. 7 shows the reference currents of the batteries in Modes 3 and 4. In Mode 3, they absorb the exceeded energy, and as soon as their SoC reaches one, the RES units change their mode to 4.

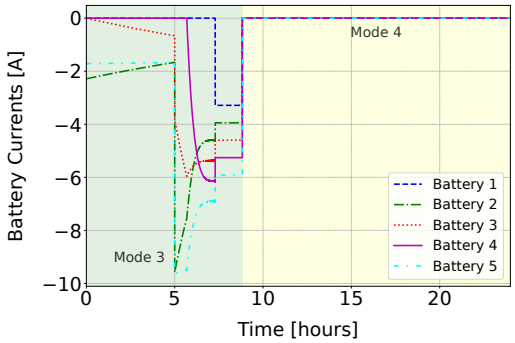

Fig. 7: Battery current in Mode 4 for $N = 5$ batteries

The produced energy in Mode 4 must exactly meet the demanded energy, which can be seen in Fig. 8. With a changing I_{demand}, the sum of the RES units follows the demanded energy.

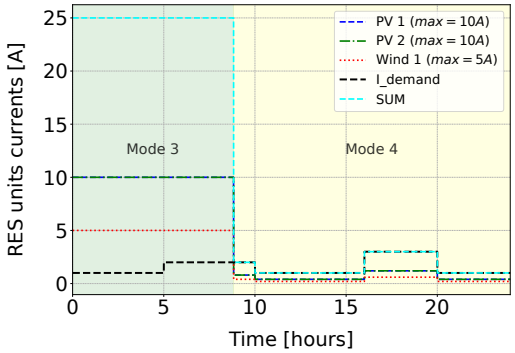

Fig. 8: Demanded and RES units' currents in Mode 4 for $M = 3$ RES units.

3) Example 3: This example illustrates the implementation of the proposed algorithm applied to a real converter transfer function. This model incorporates the details of a real converter model where its input is the duty cycle and its output is the battery current. Note that for this simulation, we considered sampling time $T_s = 0.001s$, total duration of $T = 3s$, initial $SoC = [0.5, 0.8, 0.3]$, battery capacity of $Cap = [0.01, 0.02, 0.05]$, and $N = 3$ batteries. The reason

to choose small capacities is due to avoid long simulation time. The PI controller's parameters are $k_P = 0.001$, and $k_I = 40$ which leads to a perfect tracking of the reference current with a transition time equal to 5 samples ($0.005s$). Fig. 9 demonstrates the currents that the batteries delivered as demanded by the converters. Obviously, the tracking of the current is almost perfect which shows the effectiveness of the algorithm in real-time. Mode 2 and 3 have been considered for this example. Also, Fig. 10 demonstrates the convergence of the SoCs for the batteries using the converter transfer function model.

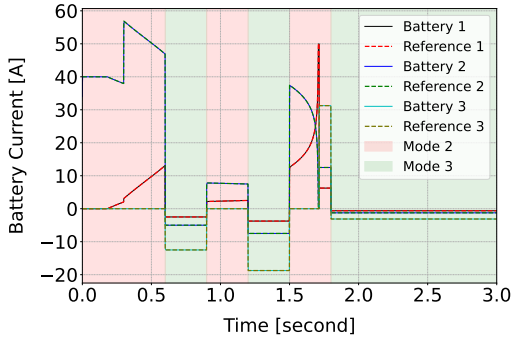

Fig. 9: The battery currents provided by the converters.

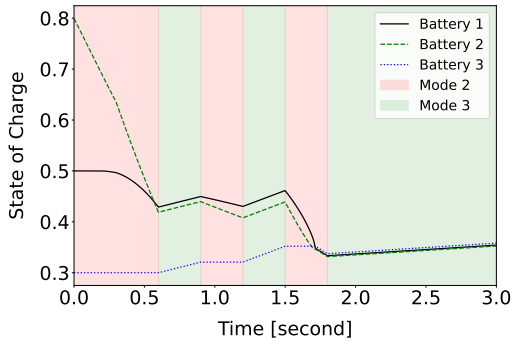

Fig. 10: The SoC convergence for the batteries working in Mode 2 and Mode 3.

Based on the Fig 9 and Fig 10, the algorithm shows a perfect tracking of the reference current in a short time while respecting the real-time constraints.

V. Conclusion

This paper presented a modified consensus-based control strategy for coordinating heterogeneous battery storage units in islanded DC microgrids. By incorporating SoC and capacity-aware coordination, together with the current term derived from DC-bus voltage signaling, the proposed approach allows balanced SoC evolution, prevents undesired battery-to-battery energy exchange, and enables effective current sharing across varying operating modes. The strategy also effectively manages periods of surplus renewable generation—particularly when all batteries are fully charged—to prevent bus overvoltage. Simulation results demonstrate that the method achieves SoC convergence, maintains supply–demand balance, and enhances battery longevity by enforcing proportional participation.

References

[1] K. Zhou, H. Yang, and F. Blaabjerg, "A review of control strategies for islanded microgrids with renewable energy sources," *Renewable and Sustainable Energy Reviews*, vol. 158, p. 112086, 2022.

[2] M. M. Islam *et al.*, "Improving reliability and stability of the power systems: A comprehensive review on the role of energy storage systems to enhance flexibility," *IEEE Access*, vol. 12, pp. 152 738–152 765, 2024.

[3] S. Ali, M. Iqbal, and M. Jamil, "Model predictive control of consensus-based energy management for dres and bess," *PLOS ONE*, vol. 18, no. 3, p. e0282224, 2023.

[4] M. R. Nasab *et al.*, "Stand-alone dc microgrids for rural areas: A decentralized energy management and voltage regulation approach," in *2024 IEEE Int. Human. Tech. Conf. (IHTC)*. IEEE, 2024, pp. 1–7.

[5] M. R. Nasab, S. Bruno, M. Liserre, and M. La Scala, "Adaptive droop control for stability enhancement in islanded dc microgrids with cpls," in *2025 IEEE Kiel PowerTech*. IEEE, 2025, pp. 1–6.

[6] S. Mohiuddin, H. Ali, and M. Hussain, "Droop-free distributed frequency control of hybrid pv–battery-based microgrids," *IEEE Transactions on Smart Grid*, vol. 13, no. 5, pp. 4075–4086, 2022.

[7] Y. Zhang, C. Li, and X. Wei, "State-of-health estimation methods for lithium-ion batteries: A comprehensive review," *Energies*, vol. 18, no. 3, p. 746, 2024.

[8] T. Dragičević, J. M. Guerrero, J. C. Vasquez, and D. Škrlec, "Supervisory control of an adaptive-droop regulated dc microgrid with battery management capability," *IEEE Transactions on power Electronics*, vol. 29, no. 2, pp. 695–706, 2013.

[9] R. Olfati-Saber, J. A. Fax, and R. M. Murray, "Consensus and cooperation in networked multi-agent systems," *Proceedings of the IEEE*, vol. 95, no. 1, pp. 215–233, 2007.

[10] T. Wang, J. He, and X. Guo, "Energy management and soc balancing of distributed batteries in ac microgrids using consensus tracking control," *Applied Energy*, vol. 363, p. 123109, 2024.

[11] M. Mosaad, A. El-Din, and A. Abdelaziz, "An enhanced consensus-based distributed secondary control for hybrid microgrids," *Frontiers in Energy Research*, vol. 11, pp. 117–129, 2023.

[12] L. Zhou, D. Du, M. Fei, K. Li, and A. Rakić, "Multiobjective distributed secondary control of battery energy storage systems in islanded ac microgrids," in *2021 40th Chinese Control Conference (CCC)*. IEEE, 2021, pp. 6981–6985.

[13] M. A. Rezaei, P. Bagheri, and F. Hashemzadeh, "Predictive consensus tracking of multi-agent systems in the presence of byzantine agents and connection loss of reference signals," *Optimal Control Applications and Methods*, vol. 45, no. 2, pp. 842–854, 2024.

[14] M. Cucuzzella, S. Trip, C. De Persis, X. Cheng, A. Ferrara, and A. van der Schaft, "A robust consensus algorithm for current sharing and voltage regulation in dc microgrids," *IEEE Transactions on Control Systems Technology*, vol. 27, no. 4, pp. 1583–1595, 2018.

[15] M. A. Rezaei, G. Manfredi, V. A. Racanelli, L. De Cicco, and S. Mascolo, "Decentralized control of uav swarms for bandwidth-aware video surveillance using nmpc," in *2024 International Conference on Unmanned Aircraft Systems (ICUAS)*. IEEE, 2024, pp. 947–954.

[16] W.-Y. Chang, "The state of charge estimating methods for battery: A review," *International Scholarly Research Notices*, vol. 2013, no. 1, p. 953792, 2013.

[17] H. Zhang, X. Tong, L. Zhang, and H. Fu, "Fast state-of-charge balancing control strategies for battery energy storage systems to maximize capacity utilization," *Journal of Energy Storage*, vol. 57, p. 106269, 2023.

[18] R. W. Erickson and D. Maksimovic, *Fundamentals of power electronics*. Springer Science & Business Media, 2007.